



Interaction of chloroquine with 2-(hydroxypropyl)- β -cyclodextrin through the supramolecular assembly for cytotoxicity on breast cancer cell lines

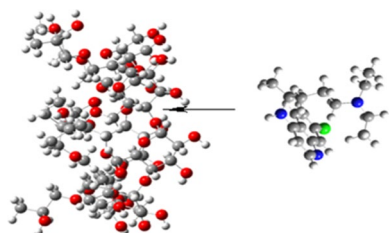
Rajaram Rajamohan¹ · Moorthiraman Murugan² · Arumugam Anitha³ · Yong Rok Lee¹ · Fatiha Madi⁴ · Nouar Leila⁴ · Muthusamy Viswalingam⁵

Received: 14 June 2022 / Accepted: 18 September 2022 / Published online: 27 September 2022
© Springer-Verlag GmbH Austria, part of Springer Nature 2022

Abstract

Our goal in the present study is to investigate the supramolecular assembly of chloroquine (CQ), with the cyclic nature of oligosaccharides, such as 2-(hydroxypropyl)- β -cyclodextrin (2HP- β -CD), in an aqueous medium. Using the BH equation, the binding constant (K) and the stoichiometric ratio between the host, 2HP- β -CD, and guest CQ are determined from the spectral changes observed in the absorption and fluorescence spectra. By employing analytical measurements such as FT-IR, SEM, powder XRD, and DSC techniques, inclusion complexes (ICs) are characterized. In addition, DFT analysis using the B3LYP/6-31G method is used to provide the structural proposal for the CQ complex with 2HP- β -CD (CQ:2HP- β -CD-ICs). Likewise, a test with cancer cell lines on the pure CQ and ICs showed no significant difference between the ICs and CQ alone in terms of cytotoxicity performances.

Graphical abstract



Keywords Chloroquine · 2-(Hydroxypropyl)- β -cyclodextrin · Inclusion complex · DFT approach · Donor–acceptor interactions · In-vitro cytotoxic assay

Rajaram Rajamohan, Moorthiraman Murugan and Arumugam Anitha have contributed equally.

✉ Rajaram Rajamohan
rajmohanau@yu.ac.kr

¹ School of Chemical Engineering, Yeungnam University, Gyeongsan 38541, Republic of Korea

² Department of Chemistry, IFET College of Engineering, Villupuram 605 108, India

³ Department of Chemistry, Government Arts College, Chidambaram 608 102, India

⁴ Laboratory of Computational Chemistry and Nanostructures, Department of Material Sciences, Faculty of Mathematical, Informatics and Material Sciences, University of 8 May 1945, Guelma, Algeria

⁵ Department of Chemistry, Periyar Maniammai Institute of Science and Technology, Thanjavur 613 403, India

Introduction

Chloroquine (CQ) is a common antimalarial drug, which prevents malaria, which is brought on by mosquito bites. Specifically, chloroquine has broad applications, including the treatment of all types of malaria infections, while it is not toxic to human leukemia cells or induces cell death in these cells [1–3]. Listed by the World Health Organization as safe and effective medicines, these drugs are essential to our health care system. Oral administration of CQ is characterized by its high bioavailability and soluble in water [4]. However, CQ has also been linked to some serious side effects [5]. Using cyclodextrins, they can be reduced by forming host–guest supramolecular assembly. Because cyclodextrins are amphiphilic, supramolecular interactions primarily occur inside the hydrophobic cavity with hydrophobic guests [6, 7].

Through host–guest systems, supramolecular chemistry describes the interaction of molecules [8]. Using weak intermolecular non-covalent bonds [9], cyclodextrins can accommodate the guest molecule and form an inclusion complex. A non-covalent interaction is commonly referred to as hydrogen bonding [10], dipole–dipole, charge transfer, van der Waals forces, and hydrophilic interactions. During the enzymatic conversion of starch to cyclodextrin, macrocyclic oligosaccharides are formed that are non-toxic [11–15]. Various forms of cyclodextrin occur naturally.

We intended to investigate the host–guest system between substituted CD instead of pure CD and small molecules, even though it gave an interesting result in biological applications. The choice of the host 2HP- β -CD is based on its availability and the cavity size [16] which is suitable for many more guest molecules. Also, natural CDs, especially β -CD, have limited water solubility as it has intra-molecular hydrogen bonds between adjacent secondary hydroxyl groups, that reduce their interactions with the water molecules [17]. 2HP- β -CD is the most widely used CD derivative and their enhanced solubilizing, amorphizing and complexing power has been well proven [18–23]. It has been demonstrated that 2HP- β -CD is safe when administered both intravenously and orally to the human body [24] and it can be used in clinical formulations to overcome poor solubility issues and enhance bioavailability [25].

We previously reported cyclodextrins' ability to form inclusion compounds via molecular encapsulation with various guest molecules [26–28]. Recently, 2HP- β -CD has been used instead of β -cyclodextrins because it has better water solubility and may be more toxicologically caring. One of the reports that correlate with our current work that clearly explained the enhancement of bioavailability and its thermodynamic parameters such as ΔH , ΔS , and ΔG are discussed for chloroquine with native CDs [2].

Recent advances in quantum chemistry have proven very useful for understanding the nature of supramolecular interactions, which play an important role in molecular properties. Theories of chemistry have focused on understanding intermolecular non-covalent interactions. Several parameters are essential in quantifying the nature of these non-covalent interactions. There are four types of parameters that can be categorized: energy decomposition analysis (EDA) [29], the analysis of atoms in molecules (AIM) [30], the analysis of non-covalent interactions (NCI) [31], and density-functional theory (DFT) [32]. DFT calculation has been a clearer to understand the interaction between guest and host via supramolecular interaction called ICs [33–36].

The ICs of CQ with 2HP- β -CD in solution and solid-state are described in this paper. We started with ICs in a liquid state and then moved on to a solid state, which we confirmed with the aid of physical and chemical analytical characterizations. DFT calculations have also been employed to derive a structural representation of the CQ:2HP- β -CD-ICs, based on the energy levels and donor–acceptor interactions. Since breast cancer has become an epidemic non-communicable disease in recent years, it has been tested on breast cancer cell lines in order to test the cytotoxic behavior of the obtained ICs.

Results and discussion

Analysis of CQ:2HP- β -CD-ICs by absorption spectra

The absorption spectra of CQ in an aqueous medium at various concentrations of 2HP- β -CD are shown in Fig. 1. CQ concentration is fixed at 1.6×10^{-5} M. The absorbance is observed as an increasing pattern with a blue shift in spectral maxima as

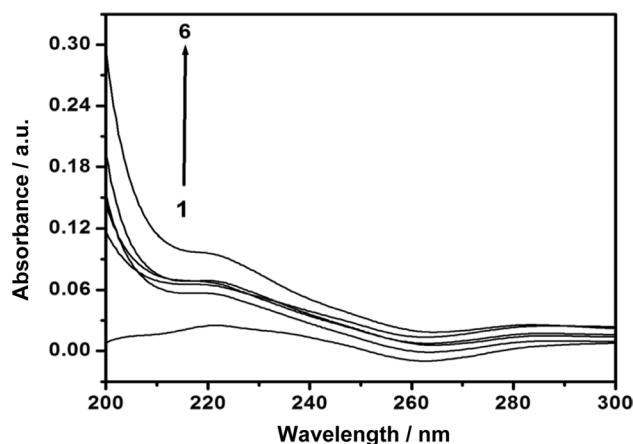
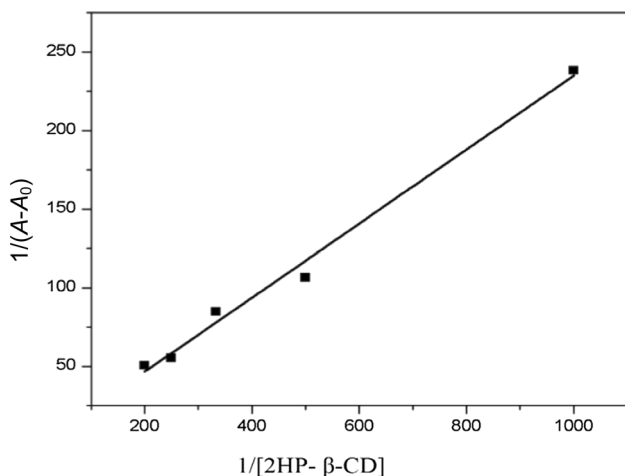


Fig. 1 Absorption spectra of CQ with increasing concentrations of 2HP- β -CD at pH 6.8 (1, 0; 2, 0.001; 3, 0.002; 4, 0.003; 5, 0.004 and 6, 0.005 M)

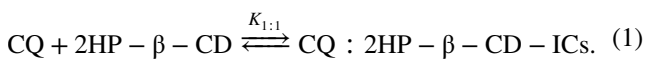
Table 1 The absorption and fluorescence spectral maxima of CQ in different concentrations of 2HP- β -CD at pH 6.8

| S.No | Conc. of 2HP- β -CD/M | Absorption spectra | | | | Fluorescence spectra | | | |
|------|-----------------------------|----------------------|----------|----------------------|----------|----------------------------|----------|----------------------------|----------|
| | | λ_{\max} /nm | Abs./a.u | λ_{\max} /nm | Abs./a.u | λ_{Flu} /nm | Int./a.u | λ_{Flu} /nm | Int./a.u |
| 1 | Without 2HP- β -CD | 221.5 | 0.0249 | 288.0 | 0.0096 | 316.0 | 86.43 | – | – |
| 2 | 0.001 | 219.5 | 0.0651 | 286.5 | 0.0147 | 316.0 | 138.26 | 351.0 | 122.89 |
| 3 | 0.002 | 219.5 | 0.0681 | 287.0 | 0.0170 | 316.0 | 159.97 | 349.0 | 164.89 |
| 4 | 0.003 | 219.0 | Shoulder | 283.5 | 0.0240 | 316.0 | 171.51 | 354.0 | 185.24 |
| 5 | 0.004 | 219.0 | Shoulder | 287.0 | 0.0245 | 316.0 | 208.4 | 354.0 | 240.41 |
| 6 | 0.005 | 218.5 | Shoulder | 284.0 | 0.0255 | 318.0 | 220.30 | 353.0 | 274.85 |

Conc. concentration, Abs. absorbance, Int. intensity

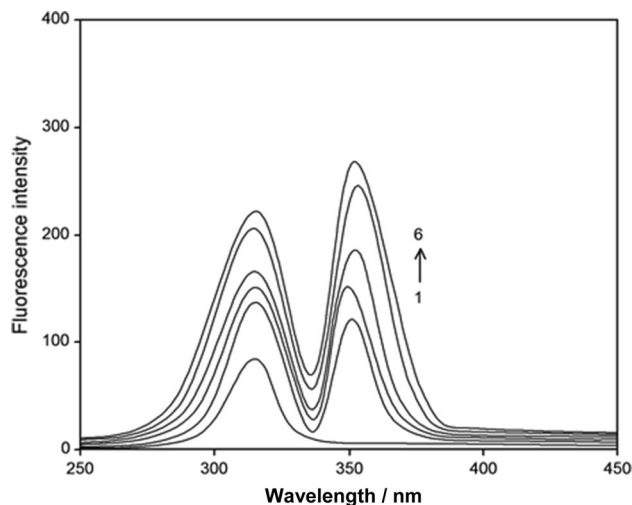
**Fig. 2** BH absorption plot of CQ with 2HP- β -CD ($\lambda_{\max} = 285.0$ nm)

the concentration of 2HP- β -CD is gradually increased until the maximum concentration of 2HP- β -CD is reached (Table 1). The host-guest interaction between CQ and 2HP- β -CD causes it to be concentration dependent with a blue shift in spectral maxima. Equation (1) depicts the equilibrium of CQ:2HP- β -CD-ICs, assuming a 1:1 complex, as follows:



The Benesi-Hildebrand (BH) equation is used to calculate the binding constant ' K ' and the stoichiometric ratio of the ICs [37, 38]. Figure 2 shows a BH absorption plot of $1/(A-A_0)$ vs. $1/[2\text{HP}-\beta\text{-CD}]$. A strong linear correlation (regression coefficient, $r^2 = 0.99$) is obtained, confirming the formation of ICs with a 1:1 stoichiometric ratio [39, 40]. Using Eq. (2), the calculated binding constant (K) at 303 K is 8.43 M^{-1} .

$$K = \frac{1}{\text{Slope}(A - A_0)}. \quad (2)$$

**Fig. 3** Fluorescence spectra of CQ with increasing concentrations of 2HP- β -CD at pH 6.8 (1, 0; 2, 0.001; 3, 0.002; 4, 0.003; 5, 0.004, and 6, 0.005 M)

Analysis of CQ:2HP- β -CD-ICs by fluorescence spectra

The fluorescence spectra of CQ at various concentrations of 2HP- β -CD in an aqueous solution are shown in Fig. 3. CQ:2HP- β -CD-ICs have a more specific effect on the fluorescence spectra of CQ than the corresponding effect on the absorption spectra. In the absence of 2HP- β -CD, CQ exhibited a single emission maximum at 316.0 nm with a fluorescence intensity of 86.43. The dual emissions are observed at 316.0 and 351.0 nm by gradually adding 2HP- β -CD. This dual emission maximum is maintained until the concentration of 0.005 M 2HP- β -CD is reached (Table 1). These modifications result in the formation of a new complex known as the ICs between CQ and 2HP- β -CD [41, 42].

The CQ molecule also allowed for excitation measurements in order to discuss and find the possibility of dual maxima in the 2HP- β -CD cavity. The CQ has an excitation spectrum at 220.0 and 286.0 nm in the absence and presence of 2HP- β -CD, respectively. These two excitation wavelengths can be seen by emitting two different wavelengths, 316.0 and 351.0 nm. The absorption spectra of CQ in the

absence and presence of 2HP- β -CD serve as the starting point for this excitation output. It is unmistakable evidence for the lack of excimer and exciplex formation with the solvents in the 2HP- β -CD medium. The BH equation is used to calculate the stoichiometry and binding constants of the CQ:2HP- β -CD-ICs, assuming a stoichiometric ratio of 1:1 [39, 40].

Figure 4 depicts a BH emission plot of $1/(I-I_0)$ versus $1/[2\text{HP-}\beta\text{-CD}]$. The plot's linearity (regression coefficient, $r^2=0.99$) suggests the formation of ICs with 1:1 stoichiometric ratio. The CQ:2HP- β -CD-ICs have a binding constant (Table 2) of 19.60 M^{-1} , and a ΔG value of -6.42 kJ/mol . The negative values of ΔG revealed indicated the formation of ICs is more than just a chemical reaction, i.e., exergonic and spontaneous at 303.0 K. Hence, the complexation process is taking place at room temperature itself and no special arrangements are required to carry out. Binding constant values are very low for these ICs obtained by both techniques because the binding process involved instant encapsulation through hydrophobic interaction between CQ and 2HP- β -CD. A similar kind of low value has been obtained for the many ICs earlier [43, 44]. However, there is a small difference in the binding constant values at the ground and excited state. The instant encapsulation enhances the binding constant value from ground to excited state.

Lifetime analysis

A lifetime analysis in a liquid state is performed to provide support for the CQ:2HP- β -CD-ICs. Figure 5 illustrates the lifetime decay of CQ with increasing concentrations of 2HP- β -CD, and Table 3 holds the respective data. The CQ molecule reveals the three-exponential decay in the aqueous medium, with three ' τ ' values (τ_1 , τ_2 , and τ_3). The

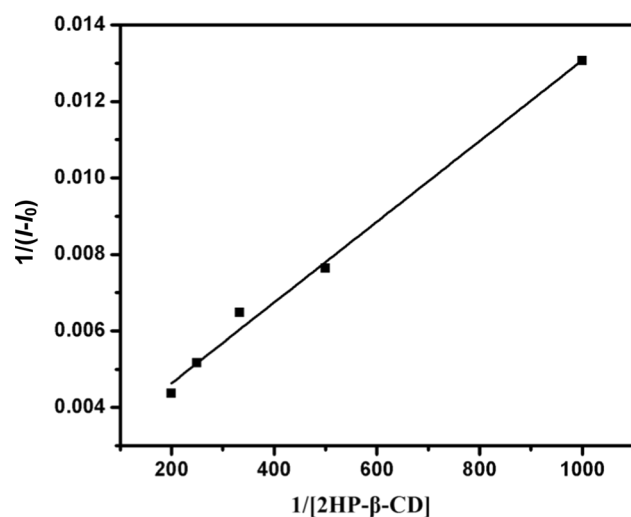


Fig. 4 BH emission plot of CQ with 1:1 ratio of ICs ($\lambda_{\text{em}}=317.0\text{ nm}$)

Table 2 Statistical parameters for the CQ:2HP- β -CD-ICs

| Parameters | Absorption spectra (λ_{abs} at 285.0 nm) | Fluorescence spectra (λ_{Flu} at 315.0 nm) |
|--------------------------|--|--|
| r^2 | 0.998 | 0.991 |
| Standard deviation | 14.84 | 21.56 |
| K/M^{-1} | 8.43 | 19.60 |
| Stoichiometry | 1:1 | 1:1 |
| $\Delta G/\text{kJ/mol}$ | -5.36 | -6.42 |

relative amplitude values are revealed that the CQ molecule is divided into three species. Upon the addition of 2HP- β -CD to the CQ, the lifetime and the relative amplitude values are increased [45–47]. The ICs have a higher amplitude than the free form of CQ. The value of χ^2 is kept at less than 1.33 for the entire analysis. The lifetime of complexed species (1) and relative amplitude are $8.89 \times 10^{-9}\text{ s}$ and 43.41%, respectively, at the highest concentration of 2HP- β -CD. The above increase in terms of lifetime and relative amplitude values is clear evidence of the formation of ICs.

Spectral analysis of CQ:2HP- β -CD-ICs

FT-IR analysis

FT-IR spectral analysis can efficiently confirm the formation of ICs [48]. A comparison of the selective and important stretching frequencies of CQ with ICs such as PM, KM, and CP may be useful in this spectral analysis. As a result of IR

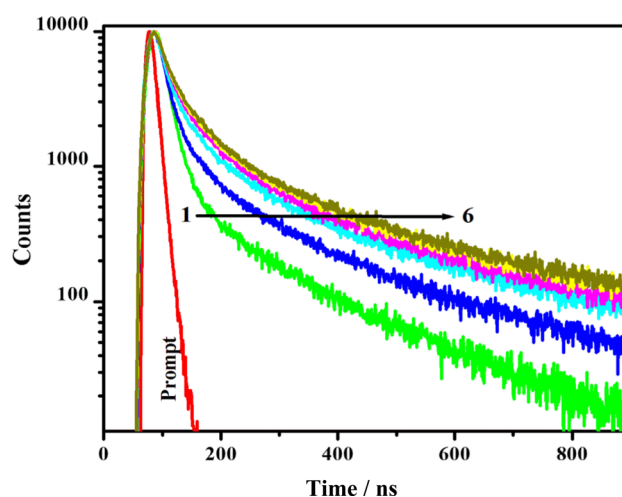


Fig. 5 Fluorescence decay curves for CQ ($1.8 \times 10^{-5}\text{ M}$) with various concentrations of 2HP- β -CD (M): 1, without 2HP- β -CD; 2, 0.001; 3, 0.002; 4, 0.003; 5, 0.004; and 6, 0.005 M

Table 3 Lifetime data of CQ with different concentrations of 2HP- β -CD ($\lambda_{\text{ex}} = 280.0$ nm, $\lambda_{\text{em}} = 315.0$ nm)

| Concentrations of 2HP- β -CD/M | Lifetime/s | Relative amplitude/% | χ^2 | Standard deviation |
|--------------------------------------|------------------------|----------------------|----------|------------------------|
| Without 2HP- β -CD | 7.34×10^{-10} | 65.65 | 1.05 | 1.44×10^{-11} |
| | 3.27×10^{-9} | 31.10 | | 2.66×10^{-10} |
| | 1.13×10^{-8} | 21.25 | | 3.39×10^{-10} |
| 0.001 | 6.76×10^{-10} | 42.08 | 1.00 | 1.31×10^{-11} |
| | 2.40×10^{-9} | 22.68 | | 8.79×10^{-11} |
| | 1.02×10^{-9} | 35.23 | | 1.65×10^{-10} |
| 0.002 | 6.48×10^{-10} | 26.53 | 1.11 | 2.62×10^{-11} |
| | 2.52×10^{-9} | 32.07 | | 2.28×10^{-11} |
| | 1.13×10^{-8} | 41.39 | | 1.69×10^{-10} |
| 0.003 | 7.04×10^{-10} | 22.70 | 1.15 | 3.09×10^{-11} |
| | 2.62×10^{-9} | 34.66 | | 6.49×10^{-11} |
| | 1.16×10^{-8} | 42.65 | | 1.78×10^{-10} |
| 0.004 | 6.68×10^{-10} | 18.80 | 0.99 | 3.22×10^{-11} |
| | 2.49×10^{-9} | 35.57 | | 2.50×10^{-9} |
| | 1.15×10^{-8} | 45.63 | | 1.48×10^{-10} |
| 0.005 | 7.70×10^{-10} | 18.74 | 1.15 | 3.61×10^{-11} |
| | 2.68×10^{-9} | 36.39 | | 6.03×10^{-11} |
| | 1.23×10^{-8} | 44.87 | | 1.91×10^{-10} |

analysis, the CP product is not simply superimposed with each other [49–51].

Table 4 shows the FT-IR spectral data for CQ, PM, KM, and CP products. Because of the stretching frequencies of an aliphatic tertiary amine, methyl group, aliphatic N–H group, and aliphatic C–H group individually, the main absorption bands of pure CQ have appeared at 1150.00, 1372.43, 766.69, and 2939.89 cm^{-1} . The above-mentioned frequencies are noticeably shifted to 1160.00, 1369.55, 760.61, and 2931.84 cm^{-1} for CP products. Also, the aliphatic C–N group and aromatic group frequencies are at 1050.04 and 3098.48 cm^{-1} , respectively, and are shifted to 1034.06 and 3080 cm^{-1} (Fig. 6). However, the stretching frequencies of the PM and KM products do not change significantly, indicating that they are less intense by the addition of 2HP- β -CD than the CP product. As a result, the CQ:2HP- β -CD-ICs have confirmed their formation in the solid state too, and

the CP process yields better ICs than the products obtained by PM and KM products.

Powder XRD analysis

Powder XRD, which is used to measure the crystallinity of the ICs, and additional evidence for the formation of ICs. The peak position (angle of diffraction) in the patterns indicates the crystal structure, and peak heights measure the crystallinity of the sample. The formation of ICs is evidenced by the formation of a diffuse diffraction pattern, the appearance of new peaks, and the disappearance of characteristic peaks of the guest molecule [52–54].

A diffractogram of CQ, PM, KM, and CP products is shown in Fig. 7. CQ exhibits a characteristic peak at 10.60°, 11.26°, 11.80°, 13.40°, 14.16°, 15.16°, 16.84°, and 17.52° revealing that the sample is crystalline in nature. The host molecule 2HP- β -CD also exhibited a distinctive peak at 2θ values and revealed the crystallinity of the sample. In the case of CP products, there is no appearance of sharp peaks with respect to either CQ or 2HP- β -CD. The sharp peaks for the CQ and 2HP- β -CD are completely merged with each other and resulted in a broader peak due to the non-crystalline and amorphous nature. Hence, these significant differences in the patterns with individual CQ (Fig. 7a) and 2HP- β -CD (Fig. 7b), may be physical evidence for the formation of ICs. However, the PM and KM products showed almost all the sharp peaks at 2θ angles and simply imitated the patterns of the pure substances of CQ and 2HP- β -CD, we strongly believed that there is an influence on the CQ molecule during the formation of ICs with 2HP- β -CD. On the whole, there are no crystalline peaks of 2HP- β -CD and CQ after ICs due to the stable interaction such as the hydrophobic interaction of CQ with 2HP- β -CD and vice versa suggests that the CQ has been reoriented to the 2HP- β -CD cavity to some extent.

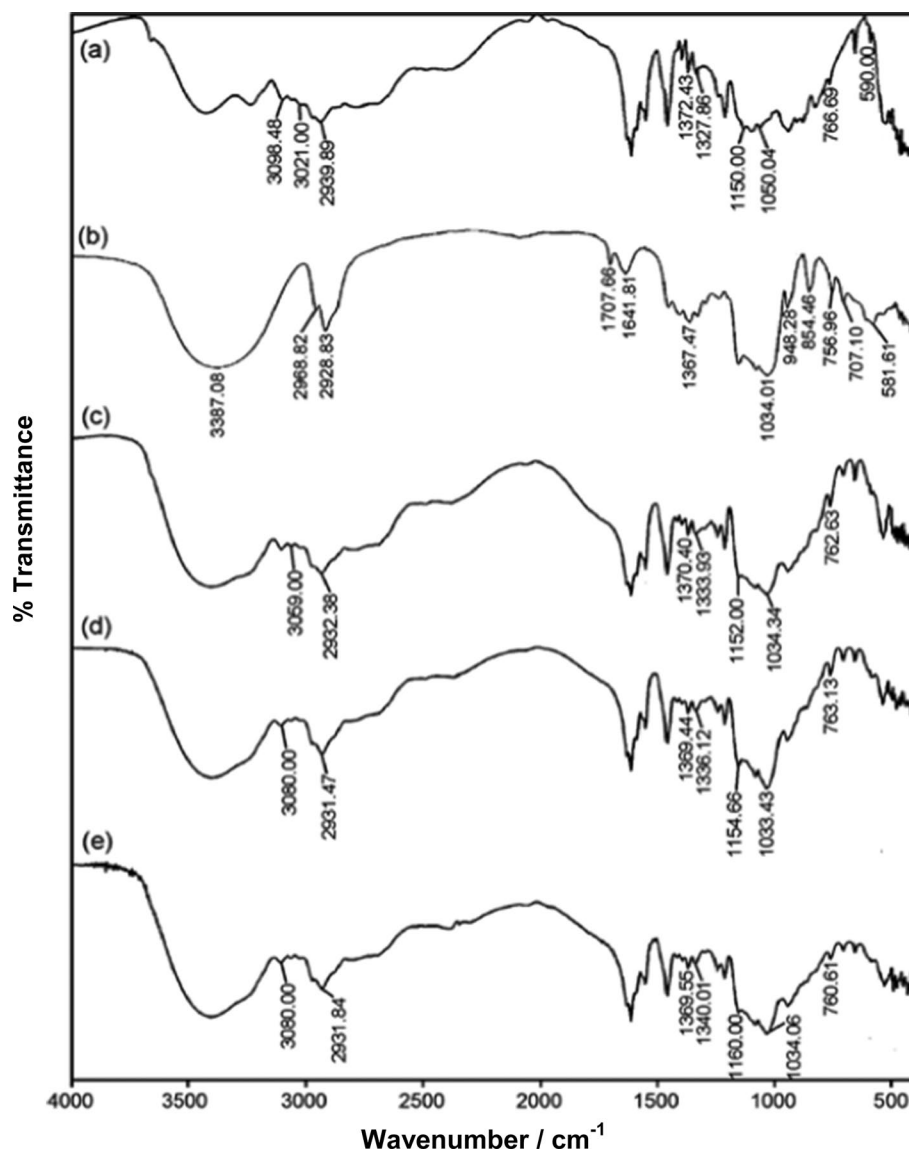
DSC analysis

DSC is one of the most reliable techniques for determining the thermal behavior of ICs such as melting, boiling, and sublimation points. Because of the inclusion of the guest

Table 4 FT-IR stretching frequencies of pure CQ, PM, KM, and CP products

| S. No | Stretching frequency | CQ/ cm^{-1} | PM/ cm^{-1} | KM/ cm^{-1} | CP/ cm^{-1} |
|-------|--------------------------|----------------------|----------------------|----------------------|----------------------|
| 1 | Aromatic C=C | 3098.48 | 3059.00 | 3080.00 | 3080.00 |
| 2 | Aromatic C–H | 3021.00 | Shoulder | Shoulder | Shoulder |
| 3 | Aliphatic C–H group | 2939.89 | 2932.38 | 2931.47 | 2931.84 |
| 4 | Aliphatic C–N | 1050.04 | 1034.34 | 1033.43 | 1034.06 |
| 5 | Aliphatic tertiary amine | 1150.00 | 1152.00 | 1154.66 | 1160.00 |
| 6 | Aliphatic N–H | 766.69 | 762.63 | 763.13 | 760.61 |
| 7 | Methyl group | 1372.43 | 1370.40 | 1369.44 | 1369.55 |

Fig. 6 FT-IR spectra of **a** CQ, **b** 2HP- β -CD, **c** PM, **d** KM, and **e** CP product



into the host cavity, the melting or boiling point of the guest may be shifted to different temperatures or vanished [50, 55]. According to this information, we can clearly explain the formation of CQ:2HP- β -CD-ICs.

The guest molecule CQ exhibits endothermic peaks at 198.93 °C, which corresponds to its melting point. This endothermic peak is compared to the standard method, such as PM, KM, and CP, which exhibit peaks at 194.11, 200.19, and 191.79 °C, respectively (Fig. 8). We can see that CP products only show a significant change in melting point, i.e., around 7.0 °C variations are observed. As a result, the CP product, rather than the PM and KM products, adequately gets CQ:2HP- β -CD-ICs.

SEM image analysis

SEM images and their interpretation provide a detailed examination of the surface morphology of the substances [37]. SEM images clearly depicted the size and shape of the ICs and their parents. Figure 9 shows SEM images of CQ, PM, KM, and CP products. The SEM images clearly show the difference between CQ and ICs. Prior to ICs, the guest molecule CQ appears to be a well-defined structure (Fig. 9a). When CQ is added to the 2HP- β -CD cavity, the rock-like structure is completely deteriorating and turned into an amorphous (Fig. 9d). Overall, the first structure of a CQ has vanished. As a result, these changes can be viewed

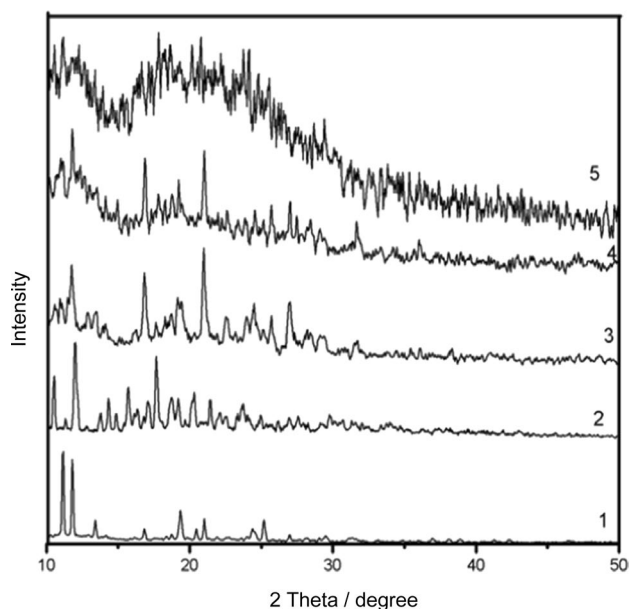


Fig. 7 Powder XRD patterns of (1) CQ, (2) 2HP- β -CD, (3) PM, (4) KM, and (5) CP product

as evidence for the formation of ICs. Though PM and KM products (Fig. 9b and c) clearly show a different morphology with CQ:2HP- β -CD-ICs, due to the cause of 2HP- β -CD. Among the three solid products (PM, KM, and CP), the CP product has the most unusual morphology of the three.

Analysis of CQ:2HP- β -CD-ICs by DFT calculations

To find a more stable structure for each angle, the energy is calculated by checking θ from -200° to 200° at 50° intervals. As the change is noticeable in dihedral points, CQ must adjust a specific conformation to form more stable ICs.

The size of the guest molecule is significant in the complexation process and plays an important role. At the same time, the guest molecule should not be too small. If it is intermolecular forces, they will not form ICs because the distance between the guest molecule and the inside of the cyclodextrin molecule is too great. On the other hand, if the large guest molecule is present, a consideration complex arrangement does not occur due to steric inhibition during the process [33–36].

Before constructing the ICs, we conducted a conformational search of the CQ guest molecule (Fig. 10). The conformational search is primarily based on varying the

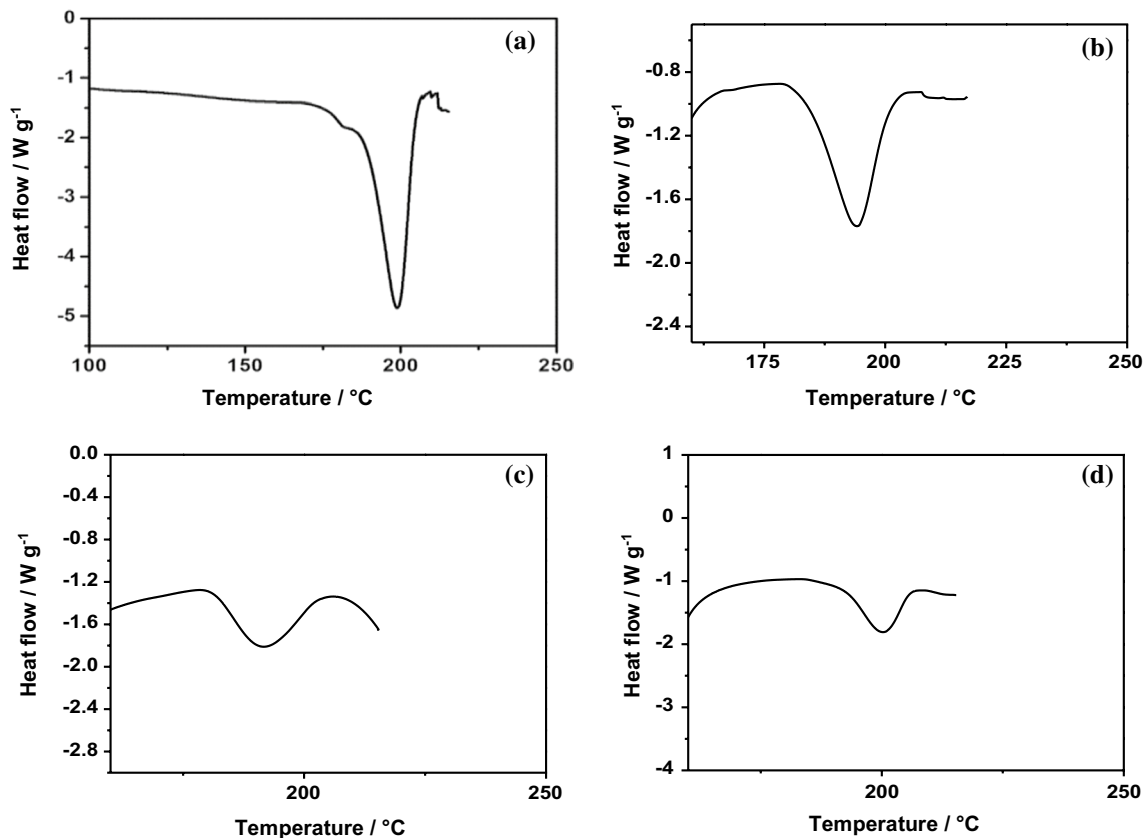


Fig. 8 DSC spectra of a CQ, b PM, c KM, and d CP products

Fig. 9 SEM images of **a** CQ, **b** PM, **c** KM, and **d** CP product

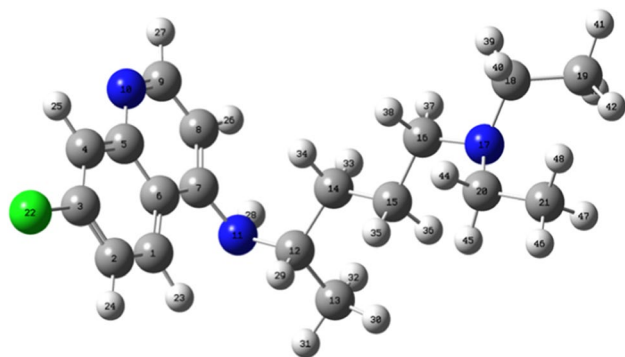
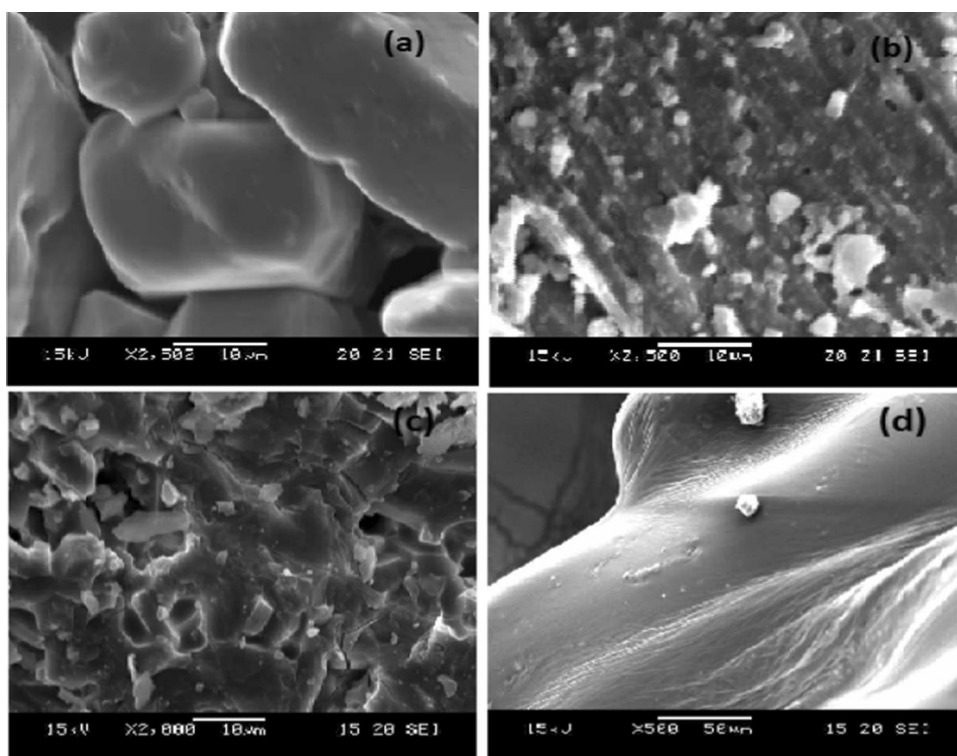


Fig. 10 CQ structure after optimization using the PM3 method

torsional angle and calculating the associated energy (Fig. 11). Five dihedral angles are considered: θ_1 ($C_7C_{11}C_{12}C_{14}$), θ_2 ($C_{12}C_{14}C_{15}C_{16}$), θ_3 ($C_{13}C_{12}C_{14}C_{15}$), θ_4 ($C_{14}C_{15}C_{16}C_{17}$), θ_5 ($C_7C_{11}C_{12}C_{13}$), and θ_6 ($C_{11}C_{12}C_{14}C_{15}$). The structure of CQ has been fully optimized for each angle using the B3LYP/6-31G (d) method.

HOMO and LUMO are important parameters in quantum chemistry. In this regard, the Δ gap (HOMO–LUMO gap) is an important scale of stability, and chemicals with large (HOMO–LUMO) values tend to be more stable. The A complex's HOMO–LUMO energy gap is projected to be 9.71 eV, which is 0.17 eV greater than the B complex (Table 5). These results show that the A orientation

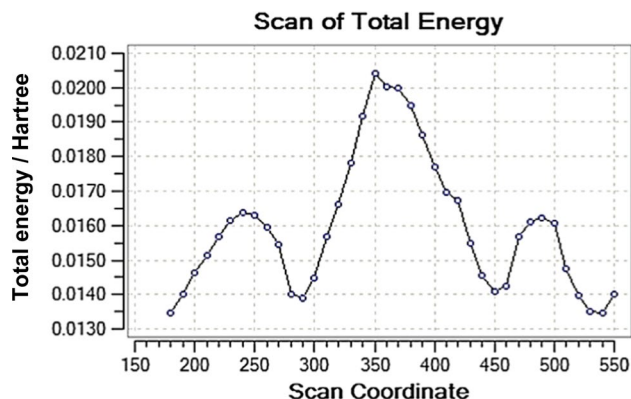


Fig. 11 Energy variation with θ_3 ($C_{13}C_{12}C_{14}C_{15}$) torsional angle by B3LYP/6-31G method

Table 5 Energies of the CQ:2HP- β -CD-ICs

| S. No | Parameters/unit | A orientation | B orientation |
|-------|-------------------------------|---------------|---------------|
| 1 | $\Delta E/\text{kJ/mol}^{-1}$ | – 81.35 | – 64.81 |
| 2 | HOMO/eV | – 8.96 | – 8.79 |
| 3 | LUMO/eV | – 0.75 | – 0.75 |
| 4 | Δ (HOMO–LUMO) | 8.21 | 8.04 |
| 5 | M/Debye | 5.89 | 5.47 |

HOMO Highest Occupied Molecular Orbital, LUMO Lowest Unoccupied Molecular Orbital

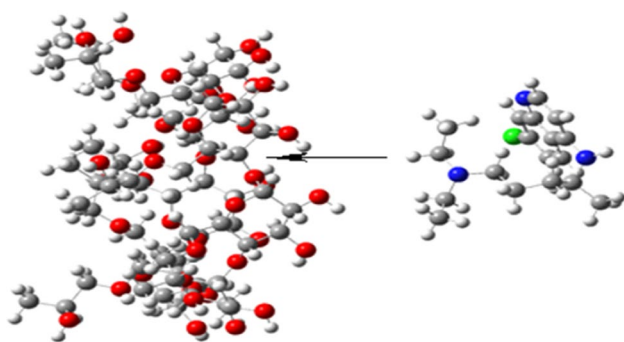


Fig. 12 The proposed structure of CQ:2HP- β -CD-ICs for A orientation

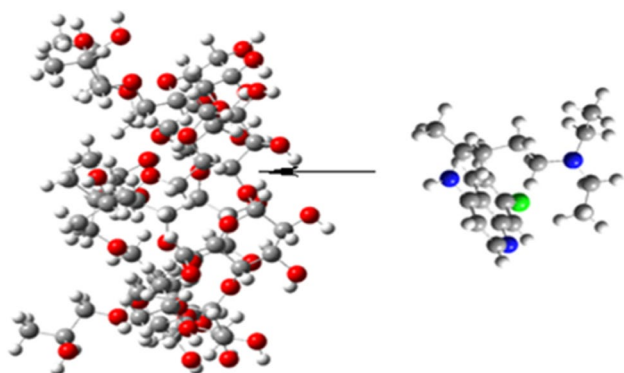


Fig. 13 The proposed structure of CQ:2HP- β -CD-ICs for B orientation

is significantly more reliable and favorable than the B orientation.

The complexation ability of 2HP- β -CD is an area with a dipole second because the boundary of 2HP- β -CD is changed and the dipole second takes on the primary role of balancing out the framed ICs. Following complexation, the variety of dipole moment of 2HP- β -CD is observed to be 5.89 and 5.47 Debye for A and B orientations, respectively (Figs. 12 and 13). As a result, the dipole moment of ICs is intimately linked to the polarity of the CQ molecule.

Tables 6 and 7 show a subset of significant donor–acceptor interactions and their stabilization energies $E^{(2)}$ calculated using the B3LYP/6-31G method. The delocalization interaction ($E^{(2)}$) ranges are 5.32–16.04 and 4.23–18.38 kJ/mol⁻¹ for CQ:2HP- β -CD-ICs with A and B orientations, respectively. The majority of σ C–H of an aliphatic group in CQ interacts with σ^* C–H of internal 2HP- β -CD, and also there is a most significant interaction observed between C 39–H 121 and σ^* C 237–H 262 (10.26 kJ/mol⁻¹) for “A” type ICs (Table 7). Furthermore, the majority of σ C–H of an aliphatic group of CQ interacts with σ^* C–H from internal 2HP- β -CD, where the important interaction is observed, as well as C 27–H 107 is also with σ^* C 221–H 242 (12.39 kJ/mol⁻¹) for “B” type ICs (Table 8). The interaction is formed between C 236–H 258 of CQ and σ^* C 27–H 107 (16.04 kJ/mol⁻¹) for “A” type ICs and vacant orbital σ^* C–H of 2HP- β -CD accepting donor C–H from the guest molecule. The important interaction for “B” type ICs is built up between donor

Table 6 Donor–acceptor interactions and stabilization energies $E^{(2)}$ (kJ/mol⁻¹) for CQ:2HP- β -CD-ICs at B3LYP/6-31G method for A orientation

| Donor | Acceptor | $E^{(2)}$ /kJ/mol B3LYP/6-31G |
|--|------------------------|----------------------------------|
| CQ:2HP- β -CD-ICs (A complex) | | |
| 2HP- β -CD proton donor and CQ proton acceptor | | |
| σ C 5–H 83 | σ^* C 238–H 263 | 8.21 |
| σ C 15–H 93 | σ^* C 232–H 252 | 6.95 |
| σ C 21–H 100 | σ^* C 236–H 259 | 10.13 |
| σ C 27–H 107 | σ^* C 236–H 258 | 8.46 |
| σ C 29–H 109 | σ^* C 235–H 257 | 9.46 |
| σ C 33–H 114 | σ^* C 235–H 256 | 8.79 |
| σ C 39–H 121 | σ^* C 237–H 262 | 10.26 |
| CQ proton donor and 2HP- β -CD proton acceptor | | |
| σ C 218–C 219 | σ^* O 74–H 138 | 5.32 |
| σ C 232–H 252 | σ^* C 15–H 93 | 9.92 |
| σ C 235–H 256 | σ^* C 33–H 114 | 11.68 |
| σ C 235–H 257 | σ^* C 29–H 109 | 11.22 |
| σ C 236–H 258 | σ^* C 27–H 107 | 16.04 |
| σ C 236–H 259 | σ^* C 21–H 100 | 12.69 |
| σ C 237–H 261 | σ^* C160–H 207 | 11.56 |
| σ C 237–H 262 | σ^* C39–H 121 | 12.60 |
| σ C 238–H 263 | σ^* C5–H 83 | 11.60 |

Table 7 Donor–acceptor interactions and stabilization energies $E^{(2)}$ (kJ/mol^{-1}) for CQ:2HP- β -CD-ICs at B3LYP/6-31G method for B orientation

| Donor | Acceptor | $E^{(2)}/\text{kJ/mol}$ B3LYP/6-31G |
|--|------------------------|--|
| CQ:2HP- β -CD-ICs (B complex) | | |
| 2HP- β -CD proton donor and CQ proton acceptor | | |
| σ C 9—H 88 | σ^* C 225—H 243 | 11.43 |
| σ C 27—H 107 | σ^* C 221—H 242 | 12.39 |
| σ O74—H 138 | σ^* C 236—H 260 | 4.23 |
| CQ proton donor and 2HP- β -CD proton acceptor | | |
| σ C 221—H 242 | σ^* C 27—H 107 | 9.76 |
| σ C 225—H 243 | σ^* C 9—H 88 | 10.93 |
| LP Cl 239 | σ^* O 64—H 134 | 18.38 |

Table 8 In-vitro cytotoxic effect of CQ and ICs on MDA MB 231 cell line

| S. no. | Name of the samples | Concentration/ $\mu\text{g/ml}$ | Inhibition/% | | | |
|--------|---------------------|------------------------------------|--------------|----------|-----------|------------------|
| | | | Trial I | Trial II | Trial III | Average |
| 1 | Control | | 98.12 | | | |
| 2 | CQ | 1000 | 89.29 | 89.03 | 89.16 | 89.16 ± 0.1 |
| | | 500 | 88.52 | 88.52 | 89.03 | 88.69 ± 0.3 |
| | | 250 | 72.96 | 75.77 | 76.91 | 75.21 ± 2.0 |
| | | 125 | 72.19 | 71.17 | 71.17 | 71.51 ± 0.6 |
| | | 62.5 | 43.62 | 45.79 | 47.58 | 45.66 ± 2.0 |
| | | CTC ₅₀ | 80 | 75 | 70 | 75 ± 5.0 |
| 3 | ICs | 1000 | 89.29 | 89.92 | 89.8 | 89.67 ± 0.3 |
| | | 500 | 91.76 | 87.04 | 87.3 | 88.7 ± 2.7 |
| | | 250 | 79.46 | 72.32 | 69.64 | 73.81 ± 5.1 |
| | | 125 | 57.53 | 53.95 | 55.23 | 55.57 ± 1.8 |
| | | 62.5 | 14.8 | 22.32 | 19.77 | 18.96 ± 3.8 |
| | | CTC ₅₀ | 115 | 120 | 120 | 118.33 ± 2.9 |

orbital C 225—H 243 and acceptor orbital σ^* C 9—H 88 ($10.93 \text{ kJ/mol}^{-1}$) of 2HP- β -CD.

One of the primary driving forces in the self-assembly and ICs is the hydrogen bond via the hydrophilic and hydrophobic interaction and it has been found in a simulation study [53]. Conformer O—H—O hydrogen bonds are recognized between σ C 218—C 219 and σ^* O 74—H 138 and with 5.32 kJ/mol^{-1} and for A complex. In addition, O—H—O hydrogen bonds with 4.23 kJ/mol^{-1} for the B complex are recognized between σ O 74—H 138 and σ^* C 236—H 260. As a result, we deduced that the connections in the A complex are the most stable because we considered energy as a primary concern, thereby proposing the most stable complex.

In-vitro cytotoxic assay

Because breast cancer is the most common cancer worldwide, the MDA MB 231 cell lines are chosen to test the

CQ:2HP- β -CD-IC's cytotoxic activity. Various concentrations (including 62.5, 125, 250, 500, and 1000 $\mu\text{g/ml}$) of pure CQ and the ICs are prepared. Upon increasing the concentration of CQ and ICs, the cytotoxicity has also changed remarkably (Table 8). Furthermore, the graph also shows clearly the changes during the assay (Fig. 14). In the ICs, the activity has been significantly improved for the concentration at 250 $\mu\text{g/ml}$ and it continued the activity hike up to a maximum concentration of 1000 $\mu\text{g/ml}$. As shown in Fig. 15, the living cells are clearly visible in the control cell (Fig. 15a). However, at higher concentrations (500 and 1000 $\mu\text{g/ml}$), the cells are elongated and 90% of the cells have died and only 10% of the cells are visible during the assay (Fig. 15b–e). Furthermore, the CTC₅₀ value is useful for activity recommendation. As a whole, CQ exhibits strong CT activity on MBA MD 231 cells, and it retains this action significantly when making it as ICs with 2HP- β -CD.

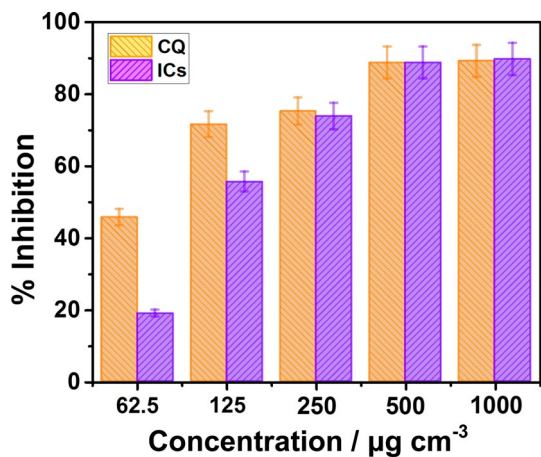
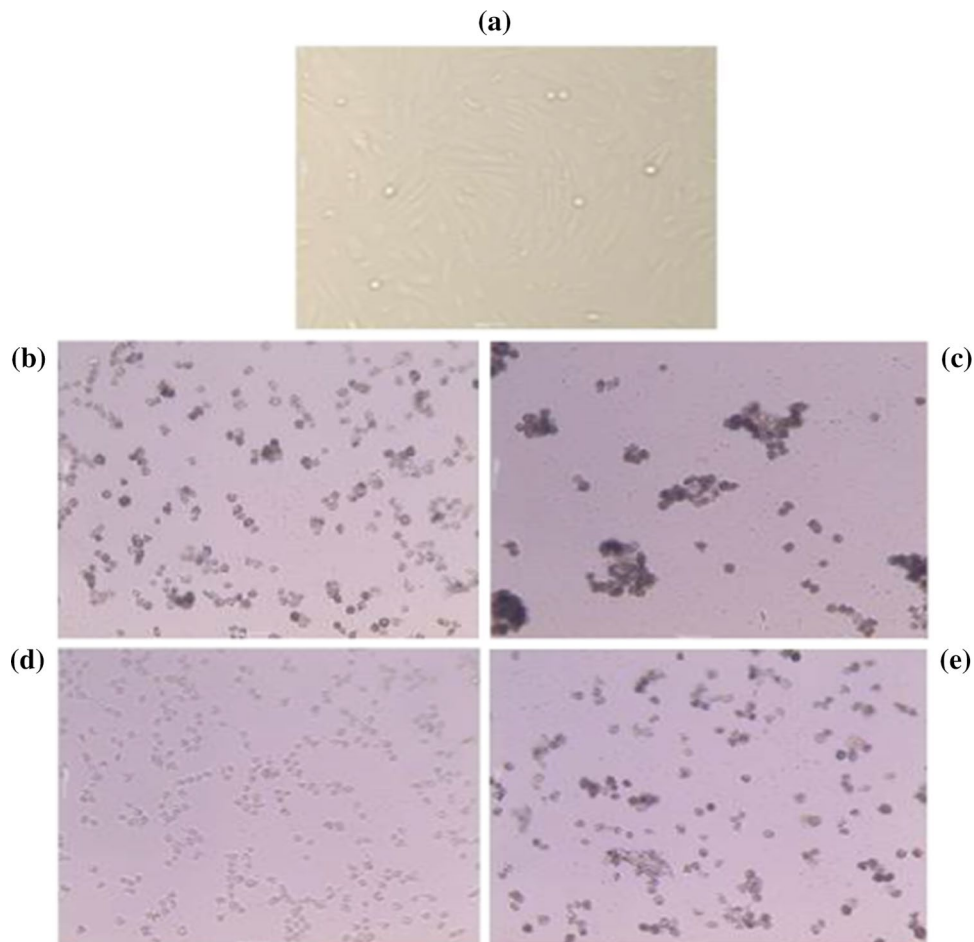


Fig. 14 Inhibition output with various concentrations for **a** CQ, **b** ICs on MDA MB 231 cell line

Conclusions

An increase in the absorbance and fluorescence intensities of the CQ molecule by the gradual addition of 2HP- β -CD

Fig. 15 CT on cell line **a** MDA MB 231 control, **b** CQ-500 C, **c** CQ-1000 C, **d** ICs-500 C and **e** ICs-1000 C



in an aqueous medium has been observed with spectral shifts occurring in both the spectral maxima. CQ:2HP- β -CD-ICs showed a dual emission maximum due to the formation of exciplex. This is evident from the effect of several solvents. A linear plot has been drawn which represented the 1:1 stoichiometric ratio for the CQ:2HP- β -CD-ICs. A strong influence is also seen on the FT-IR stretching frequencies, crystallinity, and melting behavior of CQ molecules in the CQ:2HP- β -CD-ICs. As a result of more negative complexation energy, the complexes have the favorable orientation of A over B. In-vitro cytotoxic activity of the CQ molecule is retained without any change even if it forms the stable complex (CQ:2HP- β -CD-ICs) with 2HP- β -CD.

Experimental

Sigma-Aldrich chemical company, Chennai, India, supplied CQ and 2HP- β -CD. Sigma-Aldrich chemical company, St Louis, USA, provided the 3-(4,5-dimethylthiazol-2-yl)-5-diphenyltetrazolium bromide (MTT), Fetal Bovine Serum (FBS), Phosphate Buffered Saline (PBS), Dulbecco's

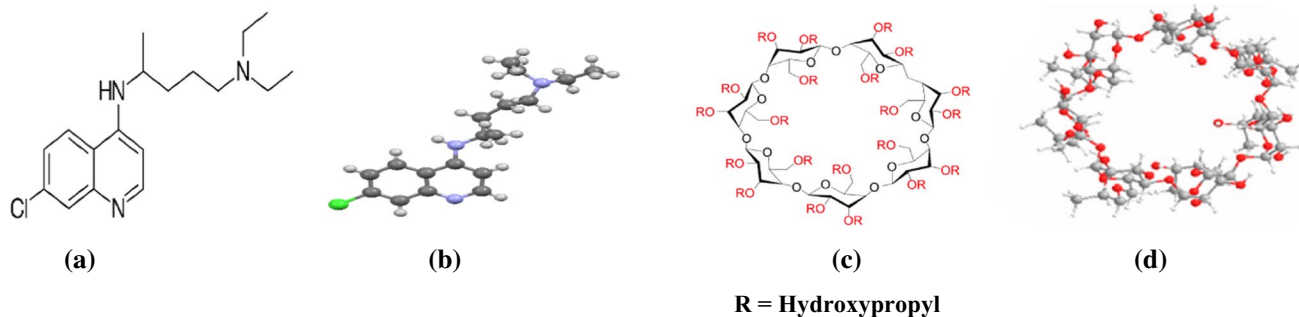


Fig. 16 Chemical structures of CQ (a & b) and 2HP- β -CD (c & d)

Modified Eagle's Medium (DMEM), and Trypsin. Hi-Media Laboratories Ltd., Mumbai, provided the EDTA, glucose, and antibiotics, which are used as such. E-Merck Ltd., Mumbai, India, supplied the dimethyl sulfoxide (DMSO) and propanol. The entire study is carried out with distilled water. The structure of guest and host has been given in Fig. 16.

Preparation of physical mixture

The required molar (1:1) quantities of the CQ and 2HP- β -CD are weighted accurately and mixed together thoroughly in a mortar, with vigorous grinding, for about three hours. These mixtures are then stored in airtight containers till further use [56]. The final dried product is denoted as PM.

Preparation of kneading products

The required quantities of the CQ and 2HP- β -CD are weighed accurately in a ratio of 1:1. A homogenous paste of 2HP- β -CD is prepared in a mortar by adding water. CQ powder is then added to this paste in portions, with continuous kneading, for three hours. An appropriate quantity of distilled water:methanol mixture (1:1) is added further to maintain the consistency of the paste. The paste is dried in a hot air oven at 100 °C for 12 h. The dried product is then powdered and stored in airtight containers till further use [56]. The final dried product is denoted as KM.

Preparation of ICs

The ICs of CQ with 2HP- β -CD are prepared using the physical mixing, kneading, and co-precipitation methods which are all described earlier [37, 38] with slight modifications in the co-precipitation method that have been employed as follows. CQ and 2HP- β -CD are precisely weighed in a 1:1 molar ratio. In water, a saturated solution of 2HP- β -CD is prepared. The CQ solution in methanol is then slowly added to it until a suspension form. The suspension is stirred for 30 min at 40 °C and then kept stirring at room temperature

for 24 h. The entire solution has allowed up to 12 h in the refrigerator for the precipitate to settle in an undisturbed environment. The solid mass is formed, and it is filtered through a 0.45 membrane filter before being dried in an oven at 110 °C for 2 h to remove the solvents associated with the solid material. The dried mass is finely ground into a fine and distinct powder before being screened through an 80-mesh sieve and stored in a safe place for further analysis and cytotoxicity test. The final dried product is denoted as CP.

Cell lines and culture medium

The cell line MDA MB 231 (Breast carcinoma) is obtained from the National Centre for Cell Sciences (NCCS) in Pune, India. Stock cells are cultured in DMEM supplemented with 10% inactivated Fetal Bovine Serum (FBS), penicillin (100 IU/cm³), streptomycin (100 g/cm³), and amphotericin B (5 g/cm³) at 37 °C in a humidified atmosphere with 5% CO₂. TPVG solution is used to dissociate the cells (mixture of 0.2% trypsin, 0.02% EDTA, and 0.05% glucose in PBS). Stock cultures are grown in 25 cm² culture flasks, and all experiments are conducted in 96 micro-titre plates (obtained from Tarsons India Pvt. Ltd., Kolkata, India).

Preparation of the solutions for cytotoxic assay

For the cytotoxicity assay, each sample is dissolved in distilled DMSO separately, and the volume is made up with DMEM supplemented with 2% inactivated FBS to obtain a stock solution with a concentration of 1 mg/cm³ and sterilized by filtration. For cytotoxic assays, serial twofold dilutions of the solution are prepared.

Instruments

The UV-Vis spectra of the solutions are recorded using a UV-1800 SHIMADZU spectrophotometer, and the fluorescence spectra are measured using an RF-5301PC

Spectrofluorimeter. The fluorescence lifetime of the solutions is measured using a single-photon counting picosecond spectrofluorimeter (TSUNAMI, SPECTRA PHYSICS, USA). FT-IR spectra are obtained using a KBr pellet and an iD1 Thermo Nicolet iS5 FT-IR spectrophotometer. The FEI Quanta FEG 200 scanning electron microscope is used for microscopic morphological measurements (SEM). Powder X-ray diffraction spectra are collected using a D8 Advance X-ray instrument (BRUKER, Germany) equipped with a 2.2 kW Cu anode, a ceramic X-ray tube as the source, a Lynx Eye (Silicon strip detector technology) as the detector, a Ni filter as the Beta filter, and a PMMA sample holder. DSC curves are generated with a Mettler Toledo DSC1HT fitted with STR software (Mettler Toledo, Switzerland). The scanning temperature range is 40–1100 °C, with a heating rate of 10 °C/min.

DFT inputs

The Hyperchem program is used to create the initial structure of CQ, and then a conformational search is performed to find the global minima of CQ. The PM3 semi-empirical method is used to examine all torsion angles, and the obtained global minima are used to develop the ICs.

The structure of 2HP- β -CD is derived from the structure of β -CD (chem3D) by replacing H of secondary hydroxyls with (C₃H₆OH), and it is then optimized using the PM3 strategy. The complex is formed by presenting the CQ in the 2HP- β -CD cavity according to two models. The PM3 optimization is used in all optimizations of the host, guest, and ICs. The calculations and result analysis are completed separately by the Gauss see and Gaussian 09 projects.

References

- Daneshfar A, Vafafard S (2009) *J Chem Eng Data* 54:2170
- Roy A, Saha S, Roy D, Bhattacharyya S, Roy MN (2020) *J Incl Phenom Macrocycl Chem* 97:65
- Kamitsuji Y, Kuroda J, Kimura S, Toyokuni S, Watanabe K, Ashihara E, Tanaka H, Yui Y, Watanabe M, Matsubara H (2008) *Cell Death Differ* 15:1712
- Furst DE (1996) *Lupus* 5:11
- Braga CB, Martins AC, Cayotopa ADE, Klein WW, Schlosser AR, Silva AF, Sousa MN, Andrade BWB, Junior JAF, Pinto WJ (2015) *Interdisc Persp Infect Dis* 2015:346853
- Carneiro SB, Duarte FIC, Heimfarth L, Quintans JSS, Quintans-Junior LJ, Junior VFV, Lima AAN (2019) *Int J Mol Sci* 20:642
- Valente AJ, Soderman O (2014) *Adv Colloid Interface Sci* 205:156
- Kyeong RR, Ji WH (2021) *Bull Korean Chem Soc* 42:1082
- Muller D, Hobza KP (2000) *Chem Rev* 100:143
- Berberan-Santos MN, Choppinet P, Fedorov A, Jullien L, Valeur B (2000) *J Am Chem Soc* 122:11876
- Umit A, Sinem ES, Yesim SK (2020) *Spectrosc Lett* 53:692
- Umit A (2021) *J Appl Spectrosc* 88:838
- Sinem ES, Umit A (2019) *J Solution Chem* 48:1535
- Umit A, Sinem ES (2018) *J Fluoresc* 28:1371
- Hye JK, Yong HC, Woo J, Ji EL (2021) *Bull Korean Chem Soc* 42:737
- Pacioni NL, Vezlia AV (2003) *Anal Chim Acta* 884:193
- Paola M (2020) *Int J Pharm* 579:119181
- Srivalli KM, Mishra B (2016) *AAPS PharmSciTech* 17:272
- Gould S, Scott RC (2005) *Food Chem Toxicol* 43:1451
- Misiuk W, Zalewska M (2009) *Carbohydr Polym* 77:482
- Folch Cano C, Yazdani-Pedram M, Olea-Azar C (2014) *Molecules* 19:14066
- Mennini N, Bragagni M, Maestrelli F, Mura P (2014) *J Pharm Biomed Anal* 89:142
- Mennini N, Cirri M, Maestrelli F, Mura P (2016) *Int J Pharm* 515:684
- Frömming K, Szejtli J (1994) *Cyclodextrins in pharmacy*. Springer, Dordrecht
- Barone JA, Moskovitz BL, Guarnieri J (1998) *Antimicrob Agents Chemother* 42:1862
- Rajamohan R, Kothai Nayaki S, Swaminathan M (2011) *J Solution Chem* 40:803
- Murugan M, Anitha A, Rajamohan R, Sivakumar K (2018) *J Solution Chem* 47:906
- Murugan M, Rajamohan R, Sivakumar K (2016) *J Macromol Sci Part A* 53:282
- Wu Y, Lucas K, Narayana RA (2016) *J Chem Phys* 144:164118
- Bader RFW (1991) *Chem Rev* 91:893
- Fuster F, Grabowski SJ (2011) *J Phys Chem A* 115:10078
- Landis CR, Weinhold F (2012) *Discovering chemistry with natural bond orbitals*. Wiley, New Jersey
- Antony Muthu Prabhu A, Fatiha M, Nouar L, Suresh Kumar GS, Sathiyaseelan K (2022). *Polycycl Arom Comp*. <https://doi.org/10.1080/10406638.2022.2101490>
- Kadri R, Djellala I, Bouhadiba A, Nouar L, Fatiha M, Guendouzi A, Gassoumi B, Lafifi I, Houari B, Oumeddour R (2022) *J Mol Struct* 1249:131565
- Amrani S, Fatiha M, Nouar L (2021) *Comp Theor Chem* 1206:113481
- Lafifi I, Nouar L, Madi F, Guendouzi A, Cheriet M, Boulaha N, Houari B (2020) *J Mol Struct* 1206:127740
- Rajamohan R, Kothai Nayaki S, Swaminathan M (2016) *J Mol Liq* 220:918
- Srinivasan K, Stalin T, Sivakumar K (2012) *Spectrochim Acta Part A* 94:89
- Anitha A, Murugan M, Rajamohan R (2018) *Spectrosc Lett* 51:198
- Hoshino M, Imamura M, Ikehara K, Hama Y (1981) *J Chem Phys* 85:1820
- Al-Hassan KA, Klei UKV, Sawaiyan A (1993) *Chem Phys Lett* 212:581
- Farcas A, Karrpiab N, Farce AM, Harbaigiu V, Guegan P (2006) *Dig J Nanomater Biostruct* 1:55
- Zielenkiewicz W, Koźbiał M, Golankiewicz B, Poznański J (2010) *J Therm Anal Calorim* 101:555
- Von Plessing RC, Sepúlveda Carreño J, Rodríguez-Baeza M, Alderete JB (2000) *Quím Nova* 23:749
- Samikannu P, Rajaram R, Krishnamoorthy S, Sharifah M (2021) *Polycycl Arom Comp* 41:992
- Rajaram R, Sundarrajulu K, Meenakshisundaram S (2017) *J Fluoresc* 27:689
- Samikannu P, Meenakshisundaram S, Krishnamoorthy S, Rajaram R (2015) *J Mol Struct* 1099:616
- Eid EED, Abdul AB, Sudari FEO, Rasedee MA (2011) *Carbohydr Polym* 83:1707
- Prabu S, Sivakumar K, Kothai Nayaki S, Rajamohan R (2016) *J Mol Liq* 219:967

50. Cid-Samamed A, Jaruporn R, Juan CM, Simal-Gandara J, Gonzalo A (2022) *Food Chem* 384:132467
51. Xinyu Z, Jianqing S, Xiaoya W, Xueyan W, Ruixue L, Xiang F, Ying L, Jiaojiao X, Xiaoli L, Rui Z, Xiuling C (2022) *Molecules* 27:2761
52. Wenzhao L, Xiaoyu L, Qingfeng Y, Ning Z, Yideng D, Huaping Z (2015) *Food Chem* 184:99
53. Veiga MD, Ahsan F (2000) *Chem Pharm Bull* 48:793
54. Fernandes CM, Vieira MT, Veiga FJB (2002) *Eur J Pharm Sci* 15:79
55. Szőri M, Jedlovsky P, Roeselová M (2010) *Phys Chem Chem Phys* 12:4604
56. Aries MJ, Moyano JR, Munoz P, Justo A (2000) *Drug Dev Ind Pharm* 26:253

Publisher's Note Springer Nature remains neutral with regard to jurisdictional claims in published maps and institutional affiliations.

Springer Nature or its licensor holds exclusive rights to this article under a publishing agreement with the author(s) or other rightsholder(s); author self-archiving of the accepted manuscript version of this article is solely governed by the terms of such publishing agreement and applicable law.